
MAGNETISM AND FERROELECTRICITY

Faraday Effect in Nanogranular Co–Sm–O Films

V. S. Zhigalov, R. D. Ivantsov, I. S. Édelman, V. A. Seredkin, G. I. Frolov, and G. V. Bondarenko

Kirensky Institute of Physics, Siberian Division, Russian Academy of Sciences, Akademgorodok, Krasnoyarsk, 660036 Russia

e-mail: zhigalov@iph.krasn.ru

Received July 14, 2004; in final form, November 2, 2004

Abstract—The Faraday effect (FE) was studied in Co–Sm–O composite films consisting of nanoparticles of metallic cobalt embedded in a samarium oxide dielectric matrix. The volume of the magnetic phase was ~60%. The FE spectral dependence for the condensates studied revealed a substantial change as compared to that for bulk cobalt samples, as well as for the films of nanocrystalline Co and CoSm films prepared in this study. An enhancement of the FE was also observed in the short-wavelength part of the optical spectrum. © 2005 Pleiades Publishing, Inc.

Composite materials made up of nanosized magnetic particles separated by a dielectric layer have considerable potential for both basic research and practical applications. The broad interest expressed in magnetic nanocomposites stems primarily from their exhibiting a number of unusual phenomena, such as giant magnetoresistance, magnetically soft and high-resistivity properties, optical transparency over a broad spectral region, and significant magneto-optical effects [1–3]. Belonging to this group is also resonant enhancement of magneto-optical effects (MOEs), which is revealed by these materials in various optical regions and was predicted by theorists (see, e.g., [4]). Because the resonance MOE originates from surface plasma vibrations in particles of the magnetic material, the MOE should depend on the particle size, the content of the magnetic phase in the composite, and the optical parameters of the metal and the dielectric. The situation is complicated by the fact that the optical and magneto-optical parameters of nanosized metal particles may differ substantially from those of the bulk materials and that the properties of composites with a high magnetic-phase content are governed both by individual characteristics of the nanoparticles and by the effects originating from their interaction.

Progress in miniaturization places a particular emphasis on film nanocomposites. The materials that have been studied thus far are primarily Co–SiO₂ film composites (see, e.g., [5, 6]). In [7], Co–Sm–O films were prepared for the first time in which a composition structure in the form of ferromagnetic nanoparticles of metallic Co embedded in a Sm oxide matrix arose under certain conditions of condensation and additional annealing. Direct observations of nanoparticles were carried out using electron microscopy and revealed some characteristic features of the magnetic properties of these composites. The results of those studies suggest that various distinctive features and magneto-optical properties could be expected in these composites,

including variations in the spectral dependence of the Faraday effect (FE).

Here, we report on a study of the spectral and field dependences of the FE in films of the Co–Sm–O system, whose structure and magnetic properties are described in [7]. The films were prepared by pulsed plasma sputtering (PPS) of a SmCo₅ target in vacuum under an initial pressure of 10⁻⁶ Torr. X-ray fluorescence analysis showed that the Sm concentration varied from one sample to another within 13–17 at. %. The samples were ~100-nm-thick and did not contain the SmCo₅ phase, because samarium has high chemical reactivity and, in the vacuum conditions chosen, oxidizes directly in the vacuum chamber in the course of film deposition. Auger electron spectroscopy detected certain amounts of carbon in the films. Electron microscopy and x-ray diffraction measurements established that the film structure is made up of magnetic particles of a Co(C) solid solution, $D \sim 1.5$ nm in size, embedded in samarium oxide (Sm₂O₃), with the volume of the magnetic phase f being ~60% [7]. This morphology of the film nanocomposite is obviously responsible for the high electrical resistivity of the samples ($\rho \sim 0.5$ Ω cm). Starting films are superparamagnetic. At room temperature, the magnetization curve has no hysteresis, but when samples are cooled, magnetic hysteresis appears, with a coercive force $H_c \cong 50$ Oe at $T = 77$ K. The temperature dependence of H_c was used to determine the blocking temperature (the temperature of transition to the superparamagnetic state), which was found to be $T_B \cong 81$ K. Our studies involved subjecting the films to heat treatment, namely, annealing in vacuum (10⁻⁶ Torr) at various temperatures, which initiated hysteresis at room temperature. The value of H_c depended on the actual annealing regime; the films subjected to short annealings at $T \leq 500$ K exhibited a weak coercive force ($H_c \leq 3$ Oe). For the purpose of comparison, we also prepared samples using the same technology of pulsed plasma

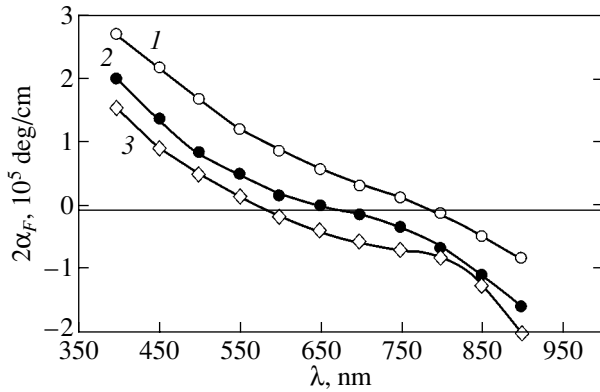


Fig. 1. Dispersion graphs of the FE ($2\alpha_F$) measured in a magnetic field $H = 4.5$ kOe for starting Co-Sm₂O₃ films on various substrates: (1) glass plates, (2) single-crystal quartz, and (3) single-crystal MgO. The effective cobalt thickness used in calculations of the specific FE was determined by x-ray fluorescence to within 5%.

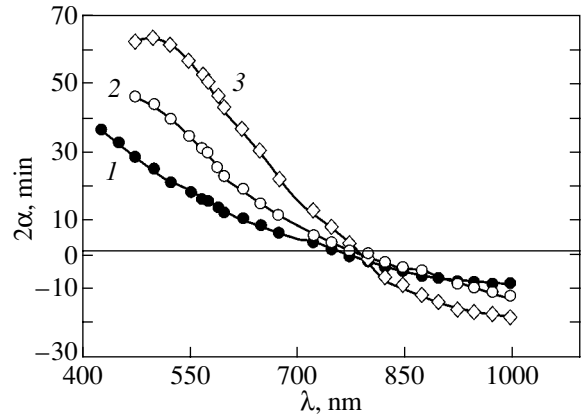


Fig. 2. Dispersion graphs of the FE ($2\alpha_F$) measured in a magnetic field $H = 4.5$ kOe for a Co-Sm₂O₃ film prepared on a glass substrate: (1) starting film and (2, 3) after annealing at (2) 520 and (3) 620 K.

sputtering of targets of pure cobalt and Co₅Sm targets in ultrahigh vacuum (10^{-9} Torr). In this case, Sm did not oxidize, as a result of which these films differed strongly from the above samples in terms of their structure and magnetic properties.

The FE spectral dependences were obtained with the null technique by modulating the plane of polarization of light in the 400- to 1000-nm spectral interval. The accuracy of measuring the rotation of the plane of polarization was $\pm 0.2'$ (Faraday rotation). A magnetic field of up to 4.5 kOe was directed along the light beam normal to the sample plane. The field was measured to within ± 20 Oe.

Figure 1 presents the FE spectral curves ($2\alpha_F$) for the starting Co-Sm₂O₃ films (thickness ~ 100 nm) deposited on different substrates. Three features immediately attract attention. (i) Unlike the decrease in the FE with decreasing wavelength of light λ in pure cobalt films reported in the literature [8], here it is seen to grow appreciably. A similar pattern was observed with the FE in layered Co/SiO₂ films [9]. (ii) the FE reverses sign in the wavelength interval from 550 to 800 nm. (iii) Single-crystal substrates are conducive to displacement of the $2\alpha_F(\lambda)$ curves toward shorter wavelengths.

Figure 2 presents $2\alpha_F(\lambda)$ graphs for films prepared on glass substrates: for the starting film (curve 1) and for those annealed at different temperatures for 30 min (curves 2, 3). We see that annealing at $T_{\text{ann}} = 620$ K brings about the appearance of a maximum near $\lambda \sim 550$ nm, with the FE increasing approximately threefold in this region. The wavelength at which the FE reverses sign does not shift. Thus, these graphs demonstrate the following points, which require explanation. First, there is a rearrangement of the FE spectrum as compared to solid Co films, which is accompanied by an enhancement of the effect in the short-wavelength region of the spectrum. Second, there is a dependence

of the FE value and of the position of the characteristic points in the spectrum on the substrate type and annealing regime.

Let us compare the FE dispersion curves obtained for a Co-Sm₂O₃ composite film with those for films prepared by ablation of metallic Co and SmCo₅ targets in ultrahigh vacuum (Fig. 3). All the films were deposited on glass substrates using the PPS technology, have the same effective thickness of the metallic component, and were annealed at 620 K. The FE spectral curves for the films prepared by ablation of a pure cobalt target or of a Co₅Sm target in a vacuum of $\sim 10^{-9}$ Torr differ in terms of their pattern from the FE graph obtained for the nanogranular Co-Sm₂O₃ film and are closer to the literature data quoted for solid Co films [8]. One can judiciously assume that the difference in the FE spectral dependences between films prepared in a higher

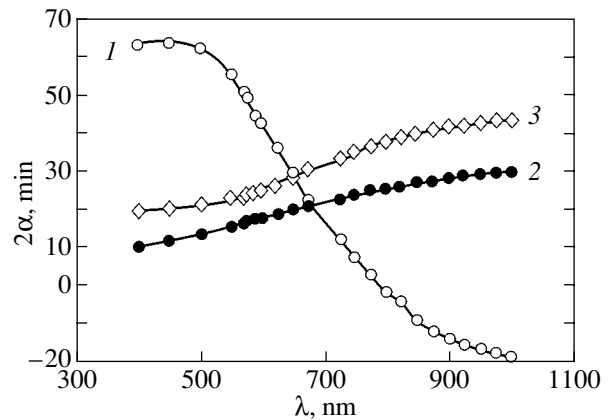


Fig. 3. Spectral curves of the FE ($2\alpha_F$) measured in a magnetic field $H = 4.5$ kOe for (1) a Co-Sm₂O₃ film and (2, 3) films prepared by ablation of (2) Co and (3) Co₅Sm targets in ultrahigh vacuum. All targets were annealed at 620 K.

and a lower vacuum originates from the formation of the Sm_2O_3 dielectric component in the latter case, which finds ready explanation in the high chemical reactivity of Sm.

As already mentioned, the observed changes in the FE wavelength dependence resemble those described to occur in multilayered Co/SiO₂ films [9], which have been interpreted satisfactorily in terms of the effective permittivity tensor [10]. As shown in [7], cobalt particles in starting films are almost spherical in shape and are distributed more or less uniformly over the bulk of the film and the linear dimension of each particle is 1.5–2.0 nm, which is about two orders of magnitude less than the film thickness (~100 nm). Therefore, in a first approximation, the effective permittivity tensor of a composite film, ϵ_{eff} , can be calculated using the model of spherical particles distributed uniformly over an infinite matrix [10]. In accordance with this model, the effective diagonal (ϵ_{eff}) and off-diagonal (γ_{eff}) components of the permittivity tensor ϵ

$$\hat{\epsilon} = \begin{bmatrix} \epsilon_{\text{eff}} & i\gamma_{\text{eff}} & 0 \\ -i\gamma_{\text{eff}} & \epsilon_{\text{eff}} & 0 \\ 0 & 0 & \epsilon_{\text{eff}}^{\parallel} \end{bmatrix} \quad (1)$$

are related to the parameters of the composite components through the relations

$$\epsilon_{\text{eff}} = \epsilon_0 \frac{2f(\epsilon - \epsilon_0) + \epsilon + 2\epsilon_0}{\epsilon(1-f) + \epsilon_0(2+f)}, \quad (2)$$

$$\epsilon_{\text{eff}}^{\parallel} = \epsilon_0 \frac{2f(\epsilon^{\parallel} - \epsilon_0) + \epsilon^{\parallel} + 2\epsilon_0}{\epsilon^{\parallel}(1-f) + \epsilon_0(2+f)}, \quad (3)$$

$$\gamma_{\text{eff}} = \frac{9f\epsilon_0^2\gamma}{[\epsilon(1-f) + \epsilon_0(2+f)]^2}, \quad (4)$$

where ϵ_0 is the permittivity of the dielectric matrix (of samarium dioxide in the case considered); ϵ and γ are the diagonal and off-diagonal components of the permittivity tensor for the particle material (cobalt), respectively; f is the magnetic-phase filling coefficient; and $N = 1/3$. We calculated the FE spectra by substituting Eqs. (2) and (4) into the well-known relation

$$\alpha_F - i\psi_F = \frac{\pi}{\lambda} \frac{\gamma}{\sqrt{\hat{\epsilon}}}. \quad (5)$$

The values of ϵ and γ were taken from [11] and [12], respectively, and it was assumed that $\epsilon_{\text{eff}} = \epsilon_{\text{eff}}^{\parallel}$. The calculation is complicated by the lack of literature data on ϵ_0 of Sm_2O_3 . Furthermore, the presence of a certain amount of carbon in the film and the small dimensions of the cobalt particles may make the optical parameters of the material of the particles substantially different from those of pure cobalt films [11]. A study of the

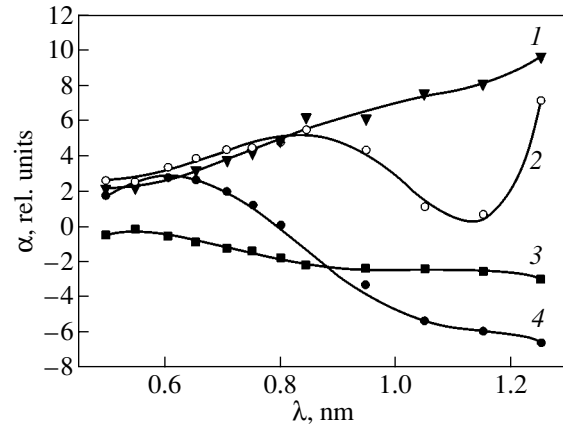


Fig. 4. FE spectral dependences calculated from Eqs. (2)–(5) for various values of the magnetic phase filling coefficient f : 1.0, 0.8, 0.6, and 0.2 (curves 1–4, respectively). The values of ϵ were taken from [11], and the values of γ , from [12] for a 26-nm-thick film [12, Table 2]; $\epsilon_0 = 4$.

parameters ϵ and γ of Co films as a function of their thickness [12] showed that variations in the film thickness have a noticeable effect on these parameters.

Figure 4 presents $\alpha(\lambda)$ graphs plotted for various values of the magnetic phase filling coefficient f . We used the values of γ' and γ'' from [12] for a film which had a value of ϵ' closest in magnitude to that given in [11]. Figure 4 demonstrates a substantial change in the FE wavelength dependence as f is varied: there appears a maximum at shorter wavelengths and the FE reverses sign. The peak value of the FE, the energy position of the maximum, and the point of reversal of the FE in sign depend nonmonotonically on f . For certain values of f , the FE remains negative throughout the spectral range covered. The FE spectral dependence calculated for $f = 0.2$ fits best to the experimental curves in Figs. 1–3. This value of f is substantially smaller than the magnetic phase filling coefficient estimated on the basis of the technological conditions. This discrepancy may be assigned to the strong misfit between the optical and magneto-optical characteristics of the particle material and the characteristics accepted in the calculation. Therefore, refining model calculations were carried out. Figure 5 plots the FE spectra calculated for $f = 0.6$ from Eqs. (2), (4), and (5) using the values of γ' and γ'' quoted in [12] for all the cobalt films with different thicknesses studied therein. Figure 6 shows variations in the FE spectral dependence with the permittivity of Sm_2O_3 . Both of these parameters are seen to have a significant effect on the FE spectra.

Another possible reason for the discrepancy between the experimental and calculated FE spectra may be the deviation of the shape of the particles from a sphere. Indeed, it was established in [13] that the magnetic moment of similar films prepared under identical conditions lies in the film plane. This is conceivable if the particles are shaped like oblate ellipsoids

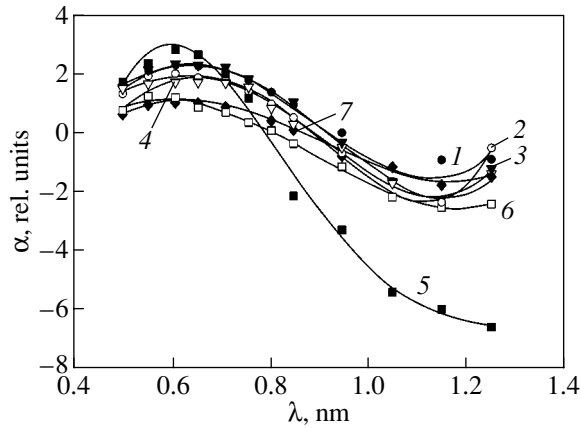


Fig. 5. FE spectral dependences calculated from Eqs. (2)–(5) for $f = 0.6$ and $\epsilon_0 = 0.4$; ϵ and γ were taken from [12, Tables 1, 2] for samples with thicknesses of 108, 58, 46, 36, 26, 22, and 13 nm (curves 1–7, respectively).

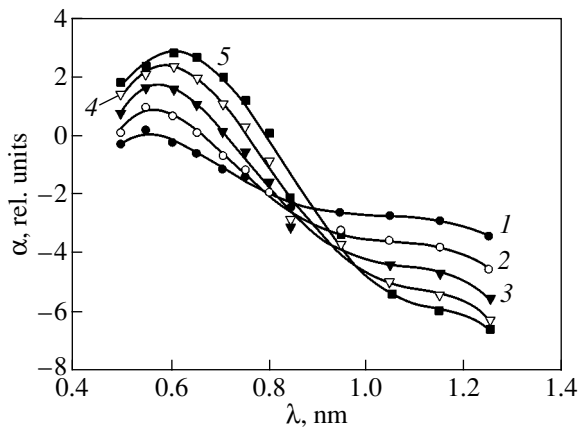


Fig. 6. FE spectral dependences calculated from Eqs. (2)–(5) for $\epsilon_0 = 2.0, 2.5, 3.0, 3.5,$ and 4.0 (curves 1–5, respectively) and $f = 0.6$. The values of ϵ and γ were taken from [12] for a 26-nm-thick film.

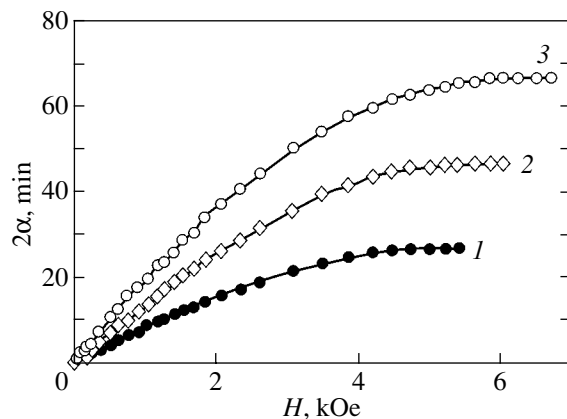


Fig. 7. Field dependences of the FE for (1) starting Co–Sm₂O₃ film and (2, 3) after annealing at (2) 520 and (3) 620 K.

with their long axes lying in the film plane. Figure 7 presents the FE field dependences plotted for the starting sample (curve 1) and samples annealed at $T_{\text{ann}} = 520$ K (curve 2) and 620 K (curve 3). Annealing increases the magnitude of the FE and its sensitivity to high magnetic fields. Note that the field dependence of magnetization for the samples described in [7] changes pattern already at a heat treatment temperature of 573 K. Assuming that the above-mentioned plane anisotropy occurs in the samples and that the size of the Co particles depends only weakly on annealing at the given temperatures [13], one can derive the effective saturation magnetization M_{eff} from the field dependence of the Faraday rotation, $\alpha = f(H_{\perp})$, by invoking the expression for the shape anisotropy field $H_S = 4\pi M_{\text{eff}}$. The values of the effective magnetization were found to be ~ 330 G for the starting film and ~ 440 and ~ 520 G after annealing for curves 2 and 3, respectively. Thus, the increase in the FE observed in annealed films can be attributed both to the growth of the effective magnetization and to a change in the optical and magneto-optical parameters of the material of the particles and/or of the matrix.

Thus, the magneto-optical properties of Co–Sm₂O₃ films with granular composite morphology, both starting and heat treated, differ strongly from those of the films of an alloy of the same elements but in the metallic state. Analogous differences were observed for these films earlier [7] in a study of the magnetic and electrical properties: the coercive force in composite films is substantially lower and the electrical resistivity is considerably higher than those for uniform metallic films prepared from the same components. One should add here the large magnitude of the FE in the short-wavelength spectral region. The possibility of fabricating nanogranular films with a large volume fraction of the magnetic phase ($\sim 60\%$) is presently attracting considerable attention for potential application.

ACKNOWLEDGMENTS

This study was supported by the Russian Foundation for Basic Research (project no. 04-02-16099-a) and the Presidium of the RAS (project no. 9.1-2004).

REFERENCES

1. F. Parent, Phys. Rev. B **55** (6), 3683 (1997).
2. D. E. Lood, J. Appl. Phys. **38** (13), 5087 (1967).
3. P. H. Lissberger and P. W. Saunders, Thin Solid Films **34** (2), 333 (1976).
4. P. M. Hui and D. Stroud, Appl. Phys. Lett. **50**, 950 (1987).
5. Yu. A. Dynnik, I. S. Édel'man, T. P. Morozova, P. D. Kim, I. A. Turpanov, and A. Ya. Beten'kova, Zh. Nauchn. Prikl. Fotogr. **43** (5), 18 (1998).
6. E. Gan'shina, A. Granovsky, B. Dieny, M. Kumaritova, and A. Yurasov, Physica B **299** (3–4), 260 (2001).
7. G. I. Frolov, V. S. Zhigalov, S. M. Zharkov, A. I. Pol'skiĭ, and V. V. Kirgizov, Fiz. Tverd. Tela (St. Petersburg) **45**

- (12), 2198 (2003) [Phys. Solid State **45** (12), 2303 (2003)].
8. K. H. Clemens and J. Jaumann, Z. Phys. **173**, 135 (1963).
9. I. S. Édel'man, T. P. Morozova, V. N. Zabluda, P. D. Kim, I. A. Turpanov, A. Ya. Beten'kova, and Yu. A. Dynnik, Pis'ma Zh. Éksp. Teor. Fiz. **63** (4), 256 (1996) [JETP Lett. **63**, 273 (1996)].
10. T. K. Xia, P. M. Hui, and D. Stroud, J. Appl. Phys. **67**, 2736 (1990).
11. P. B. Jonson and R. W. Christy, Phys. Rev. B **9**, 5056 (1974).
12. R. Carey and B. J. Thomas, Thin Solid Films **67**, L35 (1980).
13. V. S. Zhigalov, G. I. Frolov, and L. I. Kveglis, Fiz. Tverd. Tela (St. Petersburg) **40** (11), 2074 (1998) [Phys. Solid State **40** (11), 1878 (1998)].

Translated by G. Skrebtsov